

# Original synthesis of chromium (III) oxide nanoparticles

P. Gibot<sup>a,\*</sup>, L. Vidal<sup>b</sup>

<sup>a</sup> *Laboratoire Nanomatériaux pour Systèmes Sous Sollicitations Extrêmes (NS3E), ISL/CNRS UMR 3208, Institut franco-allemand de recherches de Saint-Louis (ISL), 5 rue du Général Cassagnou, F-68301 Saint Louis, France*

<sup>b</sup> *Institut de Science des Matériaux de Mulhouse (IS2 M), CNRS LRC 7228, 15 rue Jean Starcky, BP2488, F-68057 Mulhouse Cedex, France*

Received 25 May 2009; received in revised form 9 September 2009; accepted 17 September 2009

Available online 29 October 2009

## Abstract

Nanosized chromium ( $\text{Cr}_2\text{O}_3$ ) oxide was prepared by the common thermal decomposition of  $\text{Cr}(\text{NO}_3)_3 \cdot 9\text{H}_2\text{O}$  chromium (III) nitrate nonahydrate. Prior to the heat treatment at  $550^\circ\text{C}$ , the commercial reagent was first dissolved in a colloidal silica solution and then dried at a low temperature to slowly evaporate the aqueous solvent. The  $\text{SiO}_2/\text{Cr}(\text{NO}_3)_3 \cdot 9\text{H}_2\text{O}$  weight ratio ( $R$ ) was changed from 0 to 2. The various  $\text{Cr}_2\text{O}_3$  powders were characterized by XRD, FTIR, nitrogen adsorption, SEM and TEM techniques. A maximum specific surface area of  $113\text{ m}^2\text{ g}^{-1}$ , associated with a pore volume of  $0.72\text{ cm}^3\text{ g}^{-1}$ , was obtained for the  $\text{Cr}_2\text{O}_3$  powder prepared with  $R=2$ . These pristine chromium oxide nanoparticles, with a slightly sintered sphere-shaped morphology, exhibited a 10 nm particle size with a monocrystalline character as demonstrated by the TEM and XRD correlation.

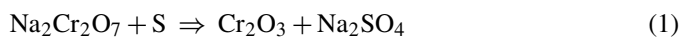
© 2009 Elsevier Ltd. All rights reserved.

**Keywords:**  $\text{Cr}_2\text{O}_3$ ; B. Nanoparticles; B. Surface; D.  $\text{SiO}_2$  spheres

## 1. Introduction

The chromium (III) oxide ( $\text{Cr}_2\text{O}_3$ ) material is being widely investigated nowadays due to its numerous application domains, including green pigments,<sup>1</sup> heterogeneous catalysts,<sup>2</sup> coating materials for thermal protection<sup>3</sup> and wear resistance.<sup>4</sup> It is considered to be an important refractory material with its high melting point temperature ( $2435^\circ\text{C}$ ) and oxidation resistance, although its sintering ability is very poor and requires special sintering conditions so that a high density can be achieved. To overcome these hindrances, the preparation of nanosized  $\text{Cr}_2\text{O}_3$  particles is currently the subject of a growing concern.

The basic and traditional process used by the manufacturers consists of reducing an alkali dichromate by sulphur, carbon, wood or ammonium chloride,<sup>5</sup> as described by the following chemical reaction:



Although simple and cheap, this process leads to the synthesis of large agglomerated particles.

In the literature many preparative techniques for  $\text{Cr}_2\text{O}_3$  nanoparticles are described, including a hard-template pathway with mesoporous silica,<sup>6</sup> hydrothermal reduction,<sup>7,8</sup> solution-combustion synthesis,<sup>9</sup> hydrazine reduction and thermal treatments,<sup>10</sup> urea-assisted homogeneous precipitation,<sup>11,12</sup> mechanochemical processing,<sup>13</sup> supercritical alcohol,<sup>14</sup> laser-induced pyrolysis,<sup>15</sup> sonochemical reaction,<sup>16</sup> microwave plasma,<sup>17</sup> condensation–polymerization process,<sup>18</sup> precipitation–gelation reaction<sup>19</sup> and gas condensation.<sup>20</sup> For most of them a large particle size distribution, low yields or important costs are the major disadvantages.

In the present study, a simple and original method for the synthesis of nanosized  $\text{Cr}_2\text{O}_3$  chromium oxide is described. This novel process involves the use of chromium (III) nitrate nonahydrate and nanometric silica spheres as chromium precursor and template agent, respectively. The surface properties, size, morphology and crystallographic structure of the as-made  $\text{Cr}_2\text{O}_3$  particles are investigated and discussed in the following sections.

## 2. Experimental

The synthesis was achieved by means of commercially available reagents without further purification. Chromium (III) nitrate

\* Corresponding author.

E-mail address: [gibot@isl.tm.fr](mailto:gibot@isl.tm.fr) (P. Gibot).

nonahydrate ( $\text{Cr}(\text{NO}_3)_3 \cdot 9\text{H}_2\text{O}$ —99%) and Ludox<sup>®</sup> HS-40 were purchased from Sigma–Aldrich. Hydrofluoric acid (40%) was obtained from Fischer Scientific.

The preparation of the chromium oxide was performed as follows: the  $\text{Cr}(\text{NO}_3)_3 \cdot 9\text{H}_2\text{O}$  reagent was dissolved in a 40% dispersion of 12-nm silica particles in water. The weight ratio of the  $\text{SiO}_2/\text{Cr}$ -based precursor ( $R$ ) was fixed at 0, 0.33, 0.66, 1 and 2. The mixtures were stirred for 1 h and dried in an oven at 80 °C to slowly evaporate the solvent. The resulting materials were slightly ground in a mortar. Then, the  $\text{SiO}_2/\text{Cr}$ -based materials were calcined in air in an oven at 550 °C for 10 min ( $2^\circ\text{C min}^{-1}$ ) in order to lead to the formation of dark green  $[\text{SiO}_2/\text{Cr}_2\text{O}_3]$  powders. To obtain nanosized  $\text{Cr}_2\text{O}_3$  materials, the calcined powders were treated twice with a diluted hydrofluoric acid solution (10%) for 2 h to remove the silica spheres. The resulting powders were centrifuged and washed several times with distilled water (until a pH higher than 5 was reached) and once with acetone. Finally, the powders were placed in an oven at 100 °C overnight.

The powder X-ray diffraction was conducted on a Bruker D8 Advance diffractometer using a  $\text{Cu K}\alpha$  radiation ( $\lambda = 1.54056 \text{ \AA}$ ) with a sol-X detector and operating at 40 kV and 40 mA. X-ray diffraction patterns were recorded between  $2\theta = 10^\circ$  and  $70^\circ$  with a step of  $0.02^\circ$  and a time of 10 s by step. The crystallographic data of the resulting  $\text{Cr}_2\text{O}_3$  powders were collected by using the FullProf Suite of the WinPLOTR software. The infrared spectra of the chromium-based powders were obtained by using a Bruker Tensor 27 spectrometer and recorded in the wave-number range of  $4000\text{--}500 \text{ cm}^{-1}$  by superposing 20 scans and with a resolution of  $4 \text{ cm}^{-1}$ . Nitrogen isotherm measurements were performed on a Beckman Coulter SA 3100 surface area analyzer at 77 K and on samples (of approximately 0.2 g) previously outgassed at 423 K for 10 h. The specific surface area ( $S_{\text{BET}}$ ) was determined according to the Brunauer–Emmet–Teller (BET) method in the 0–0.25 relative pressure range. The pore size distribution was obtained by following the Barret–Joyner–Halenda (BJH) approach. The scanning and transmission electronic microscopy investigations were carried out on a DSM 982 Gemini (Zeiss) and a CM200 (Philips) devices, respectively.

### 3. Results and discussion

The process developed in the present study is based in the utilization of the interstitial spaces of a silica building as nano-reactors for the synthesis of inorganic nanoparticles. In our case,

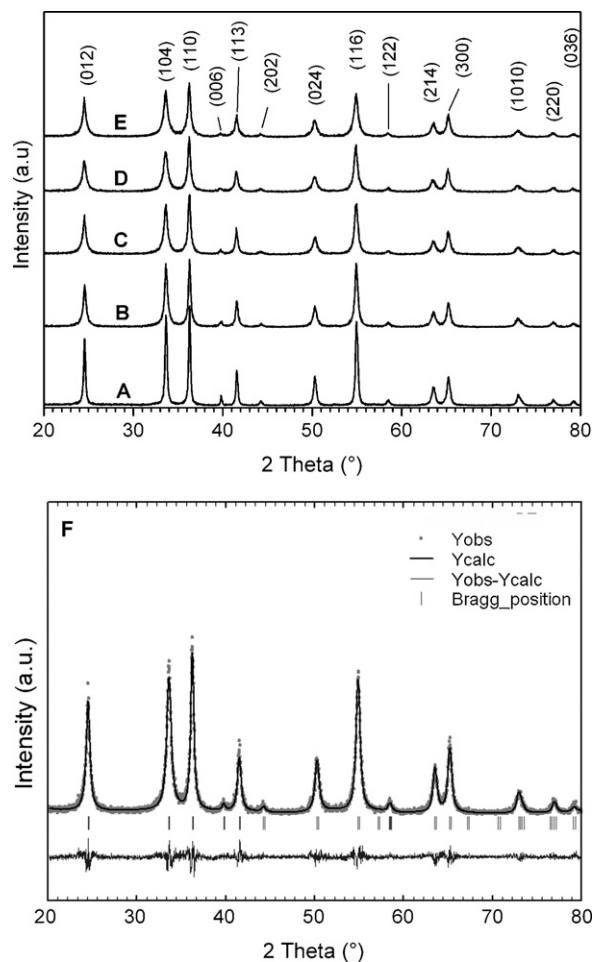


Fig. 1. XRD patterns of the chromium (III) oxide powders synthesized with (A)  $R=0$ , (B)  $R=1/3$ , (C)  $R=2/3$ , (D)  $R=1$  and (E)  $R=2$  ( $R$  represents the silica spheres/chromium precursor weight ratio). The graph (F) corresponds to the refinement results of the  $\text{Cr}_2\text{O}_3$  powder synthesized with  $R=2$ .

the elaboration of a building template is based on the capacity of silica nanospheres, dispersed in an aqueous solution, to self-assemble into different packing domains (simple cubic packing, face-centred cubic or hexagonal close packing) from the liquid phase removal by evaporation. The most probable packing is the hexagonal one with the elaboration of tetrahedral or octahedral interstitial spaces. In the case of tetrahedral sites as reactor, the synthesis of oxide particles with the smallest nanoscale diameter ( $r_{\text{oxide}} = 0.225 \times r_{\text{SiO}_2}$ ) may be considering.

The XRD patterns of the powders obtained after calcination, acid etching and with various  $R$  values are shown in Fig. 1A–E.

Table 1  
Crystallographic data of the different synthesized  $\text{Cr}_2\text{O}_3$  powders.

	Reference 072-3533	As-prepared $\text{Cr}_2\text{O}_3$ samples with $R =$				
		0	1/3	2/3	1	2
$a$ (Å)	4.953	4.953	4.956	4.953	4.957	4.954
$c$ (Å)	13.578	13.582	13.593	13.593	13.604	13.597
$\gamma$ (°)	120.00	120.00	120.00	120.00	120.00	120.00
$V$ (Å <sup>3</sup> )	288.47	288.65	289.23	288.86	289.53	289.08
$D_{50}$ (nm)	–	$35 \pm 9$	$19 \pm 4$	$17 \pm 5$	$14 \pm 4$	$12 \pm 2$

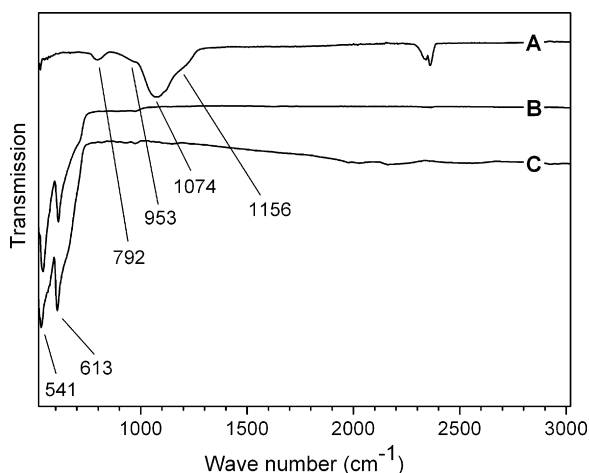


Fig. 2. Infrared spectra of (A) the  $\text{SiO}_2$  nanosphere reagent, (B) the as-synthesized  $\text{Cr}_2\text{O}_3$  powder ( $R=2$ ) after acid etching and finally (C) a commercial  $\text{Cr}_2\text{O}_3$ .

In all cases, the as-prepared samples were identified as pure well-crystallized  $\text{Cr}_2\text{O}_3$  chromium (III) oxide. No impurities or silica traces were detected. The diffraction peaks were indexed in the rhombohedral system with an  $R\text{-}3c$  space group, as described in the 072-3533 JCPDS card. The crystallographic data of each pristine  $\text{Cr}_2\text{O}_3$  samples, realized with the FullProf Suite of the WinPLOTR software are gathered in Table 1. A  $\text{LaB}_6$  reference powder measured in the same diffraction conditions was used to correct for instrumental broadening. The data are very similar to the theoretical values, thus suggesting a good stoichiometry of all the synthesized chromium (III) oxide samples. The crystallite size of each sample was estimated from the refined parameters describing the diffraction profile using the Scherrer formula. The following trend was observed: the higher the  $R$  value is, the smaller the crystallite sizes are. The result can be easily explained by the fact that the more silica spheres there are for the same given product mass, the fewer the available interstitial spaces enabling to precipitate the well-crystallized  $\text{Cr}_2\text{O}_3$  particles.

Fig. 2 shows the infrared spectra of the silica nanosphere precursor, one of the as-made samples ( $R=2$ ) after acid etching and a commercial chromium (III) oxide. For all spectra, no nitrate specie was detected ( $\sim 1095\text{ cm}^{-1}$ ). On the spectrum A, four vibration bands at 792, 953, 1074 and  $1184\text{ cm}^{-1}$  were detected. These are known to be characteristic of the vibrations of the Si–O–Si species, as reported in the literature.<sup>21</sup> From the spectrum C, the large domain located between 500 and  $700\text{ cm}^{-1}$  was attributed to the vibration band of the metal–oxide links; the vibration band at  $541\text{ cm}^{-1}$  characterizes the Cr–O distortion vibration and the band at  $613\text{ cm}^{-1}$  identifies the chromium oxide as the  $\text{Cr}_2\text{O}_3$  phase.<sup>22</sup> The C spectrum, which characterizes the as-synthesized  $\text{Cr}_2\text{O}_3$  samples ( $R=2$ ) after the acid etching, only reveals the corresponding vibration bands of Cr–O links suggesting the successful removal of the silica template agent and the high purity of the as-synthesized  $\text{Cr}_2\text{O}_3$  particles.

The nitrogen adsorption/desorption investigations were carried out on all the  $\text{Cr}_2\text{O}_3$  powders. Fig. 3A shows the nitrogen sorption isotherms obtained for the four/five as-made samples. The numerous profiles correspond to a IV-type adsorptive isothermal curve, on which a hysteresis loop can be observed, suggesting the presence of a porous structure and more precisely a mesoporous structure. For all samples, above the relative pressure of 0.9, the isotherms still rise, indicating that the chromium-based samples also exhibit a macroporous structure. For each synthesized oxide, the BET method was employed to calculate the specific surface area and the total pore volume was estimated from the amount adsorbed at a relative pressure of 0.9814. From the desorption curve, the BJH method was used to determine the pore size distributions (Fig. 3B). All data relating to the surface properties are gathered in Table 2. As the  $R$  ratio increases from 0 to 2, the specific surface area and pore volume of the different  $\text{Cr}_2\text{O}_3$  powders prepared increase from  $10.5$  to  $113\text{ m}^2\text{ g}^{-1}$  and from  $0.045$  to  $0.72\text{ cm}^3\text{ g}^{-1}$ , respectively. To our knowledge, this is the first time such values are found for well-crystallized chromium (III) oxide phases. As shown on Fig. 3B, the pore size distribution of all  $\text{Cr}_2\text{O}_3$  samples reveals a large pore distribution with, only for the sample synthesized with  $R=1/3$ , a peak at  $10\text{--}12\text{ nm}$  characteristic of the

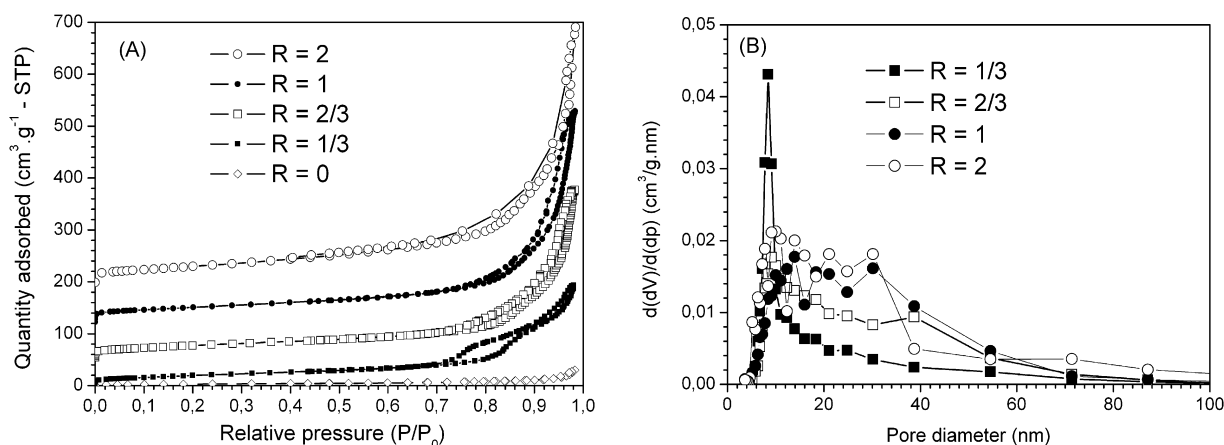


Fig. 3. (A) Nitrogen adsorption–desorption isotherms and (B) pore size distributions of the chromium (III) oxide powders synthesized with various  $R$  values. The isotherms were set up for a better legibility. ( $R$  represents the silica spheres/chromium precursor weight ratio.)

Table 2

Surface properties of the different synthesized  $\text{Cr}_2\text{O}_3$  powders ( $R$  representing the silica spheres/chromium precursor weight ratio).

	As-prepared $\text{Cr}_2\text{O}_3$ samples with $R =$				
	0	1/3	2/3	1	2
$S_{\text{BET}}$ ( $\text{m}^2 \text{g}^{-1}$ )	10.42	71.97	85.65	101.56	113
Pore volume ( $\text{cm}^3 \text{g}^{-1}$ )	0.04	0.39	0.49	0.61	0.72
Pore size (nm)	–	10–12	10–50	10–50	10–50
Particle size (nm)	110	16	14	12	10

silica sphere average diameter. These large pore size distributions confirm the existence of a macroporous structure (pore diameter  $> 50$  nm) as was previously supposed from isotherm profiles. No microporous surfaces or volumes were determined for all the synthesized chromium oxides.

The representative scanning and transmission microscope images of two as-prepared  $\text{Cr}_2\text{O}_3$  powders ( $R = 0$  and 2) are displayed in Fig. 4. In a general way, highly agglomerated particles are observed in both cases. For  $R = 0$  (Fig. 4A and B), the particle size was changed from 40 nm to 0.4  $\mu\text{m}$  and an undefined shape morphology can be observed. The particle size of chromium (III) oxide was decreased proportionally to the increase of the  $R$  value as for  $R = 2$ , 10 nm-sized spherical particles were noted (Fig. 4C

and D). In Fig. 4D, the particles are bonded by chromium oxide bridges which could be likened to a replica of the interstitial space that exists in a regular arrangement of balls. These electronic observations are in good agreement with the average particle size deduced from the BET specific surface area measurements (Table 2) with the following formula:  $d = 6/\rho A$ , where  $\rho$  is the theoretical density of the particles ( $5.21 \text{ g cm}^{-3}$ ) and  $A$  the specific surface area, and the crystallite size determined from the X-ray analysis (Table 1). This correlation makes it possible to suggest the monocrystalline character of the synthesized  $\text{Cr}_2\text{O}_3$  nanoparticles.

In summary, the smaller particle size for the  $\text{Cr}_2\text{O}_3$  particles synthesized, from this new process, is of 10 nm with a

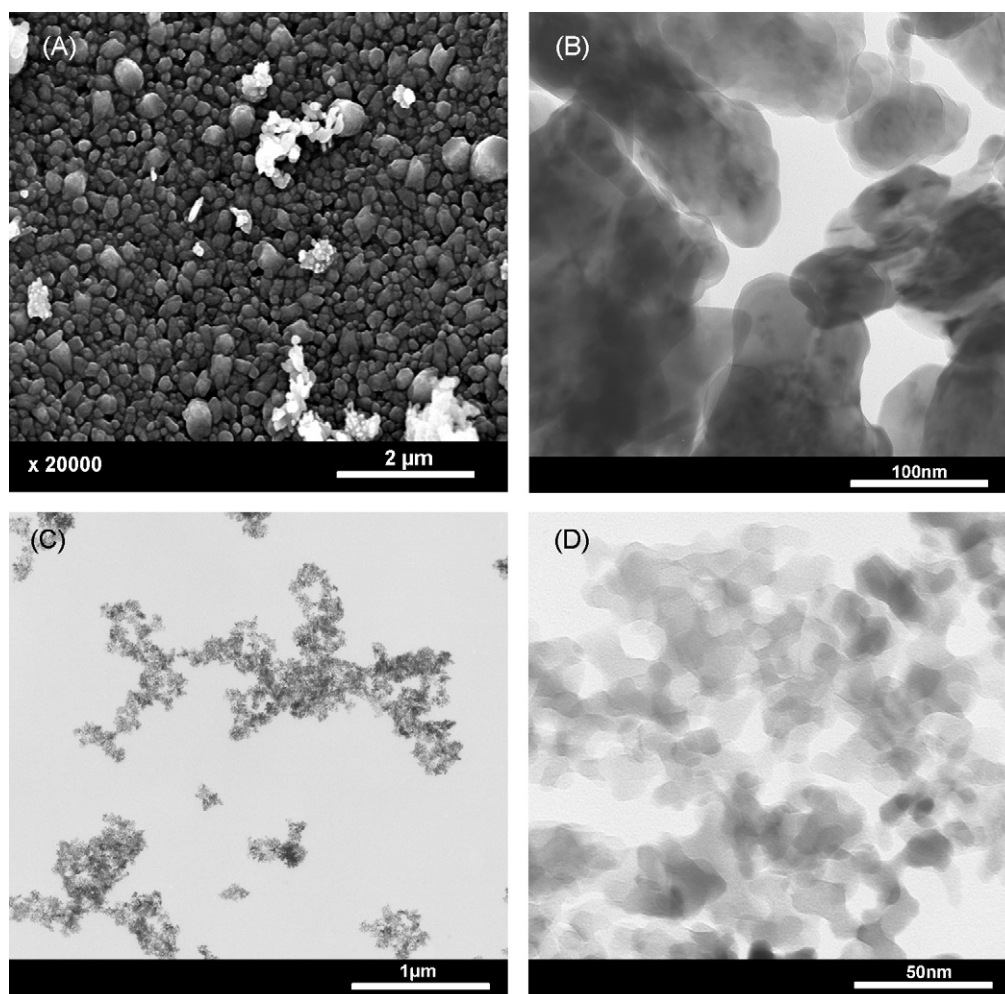


Fig. 4. SEM and TEM images of the  $\text{Cr}_2\text{O}_3$  powders synthesized from (A and B)  $R = 0$  and (C and D)  $R = 2$ .

SiO<sub>2</sub>/chromium precursor molar ratio of 2. With higher value, indeed 3 (not presented and discussed in the paper) the same value of 10 nm was found. For us, the results suggest that the packing of the silica balls during the evaporation of the solvent is not optimal with our procedure and consequently the interstitial spaces created are bigger than the wished ones ( $r_{\text{oxide}} = 0.225 \times r_{\text{SiO}_2}$ ). A faster and forced evaporation of the solvent can be suggested to explain this result. An evaporation procedure of the solvent of several weeks would be more efficient to correctly arrange the silica balls so allowing the formation of smallest interstitial and consequently the synthesis of Cr<sub>2</sub>O<sub>3</sub> particles with size less than 10 nm.

#### 4. Conclusion

Chromium trioxide Cr<sub>2</sub>O<sub>3</sub> nanoparticles were successfully synthesized via an easy and fast route by using an aqueous dispersion of nanosized silica spheres as template agent. With a [silica/chromium precursor] weight ratio equal to 2, the chromium (III) oxide powder with a specific surface area and a pore volume of 113 m<sup>2</sup> g<sup>-1</sup> and 0.72 cm<sup>3</sup> g<sup>-1</sup>, respectively, was synthesized. This sample is composed of highly agglomerated nanoparticles with an average diameter of 10 nm. To our knowledge, this is the first time that such interesting values are published for a chromium (III) oxide material. These high surface area Cr<sub>2</sub>O<sub>3</sub> powders are currently tested in our laboratory, in particular in the preparation of energetic composites used in the pyrotechnic domain. In a more global way, the synthesis strategy used herein could be easily extended to the formation of other inorganic nanomaterials.

#### Acknowledgments

The authors are grateful to Dr. Denis Spitzer for fruitful discussions.

#### References

1. Brock, T., Groteklaes, M. and Mischke, P., *European Coating Handbook*. Vincentz Verla, Hanover, Germany, 2000, p. 133.
2. Abu-Zied, B. M., Structural and catalytic studies of silver/chromia catalysts. *Appl. Catal. A: Gen.*, 2000, **198**, 139–153.
3. Berdhal, P., *Trans. Am. Soc. Mech. Eng. J. Heat Transfer*, 1995, **117**, 355–358.
4. Kitsunai, H., Hokkirigawa, K., Tsumaki, N. and Kato, K., Transitions of microscopic wear mechanism for Cr<sub>2</sub>O<sub>3</sub> ceramic coatings during repeated sliding observed in a scanning electron microscope tribosystem. *Wear*, 1991, **151**, 279–289.
5. Tsuzuki, T. and McCormick, P. G., Synthesis of Cr<sub>2</sub>O<sub>3</sub> nanoparticles by mechanochemical processing. *Acta Mater.*, 2000, **48**, 2795–2801.
6. Wang, Y., Yuan, X., Liu, X., Ren, J., Tong, W., Wang, Y. and Lu, G., Mesoporous single crystal Cr<sub>2</sub>O<sub>3</sub>: synthesis, characterizations, and its activity in toluene removal. *Solid State Sci.*, 2008, **10**, 1117–1123.
7. Pei, Z., Xu, H. and Chang, Y., Preparation of Cr<sub>2</sub>O<sub>3</sub> nanoparticles via C<sub>2</sub>H<sub>5</sub>OH hydrothermal reduction. *J. Alloys Compd.*, 2008, **468**, L5–L8.
8. Pei, Z. and Zhang, Y., A novel method to prepare Cr<sub>2</sub>O<sub>3</sub> nanoparticles. *Mater. Lett.*, 2008, **62**, 504–506.
9. Lima, M. D., Bonadimann, R., de Andrade, M. J., Toniolo, J. C. and Bergmann, C. P., Nanocrystalline Cr<sub>2</sub>O<sub>3</sub> and amorphous CrO<sub>3</sub> produced by solution combustion synthesis. *J. Eur. Ceram. Soc.*, 2006, **26**(7), 1213–1220.
10. Gui, Z., Fan, R., Mo, W., Chen, X., Yang, L. and Hu, U., Synthesis and characterizations of reduced transition metal oxide and nanophase metals with hydrazine in aqueous solution. *Mater. Res. Bull.*, 2003, **38**, 169–176.
11. Wolfowich, M. A., Rotter, H., Landau, M. V., Korin, E., Erenburg, A. I., Mogilyansky, D. and Gartstein, D. E., Texture and nanostructure of chromium aerogels prepared by urea-assisted homogeneous precipitation and low temperature supercritical drying. *J. Non-Cryst. Solids*, 2003, **318**, 95–111.
12. Ocana, M., Nanosized Cr<sub>2</sub>O<sub>3</sub> hydrates spherical particles prepared by the urea method. *J. Eur. Ceram. Soc.*, 2001, **21**, 931–939.
13. Tsuzuki, T. and McCormick, P. G., Synthesis of Cr<sub>2</sub>O<sub>3</sub> nanoparticles by mechanochemical processing. *Acta Mater.*, 2000, **48**(11), 2795–2801.
14. Znaidi, L. and Pommier, C., Synthesis of nanometric chromium (III) oxide powders in supercritical alcohol. *Eur. J. Solid State Inorg. Chem.*, 1998, **35**(6–7), 405–417.
15. Peters, G., Jerg, K. and Schramm, S., Characterizations of chromium (III) oxide powders by laser-induced pyrolysis of chromyl chloride. *Mater. Chem. Phys.*, 1998, **55**, 197–201.
16. Arul Dash, N., Koltypin, Y. and Gedanken, A., Sonochemical preparation and characterizations of ultrafine chromium oxide and manganese oxide powders. *Chem. Mater.*, 1997, **9**, 3159–3163.
17. Vollath, D., Szabo, D. V. and Willis, J. O., Magnetic properties of nanocrystalline Cr<sub>2</sub>O<sub>3</sub> synthesized in a microwave plasma. *Mater. Lett.*, 1996, **29**(4–6), 271–279.
18. Kawabata, A., Yoshinaka, M., Hirota, K. and Yamaguchi, O., Hot isostatic pressing and characterizations of the sol–gel derived chromium (III) oxide. *J. Am. Ceram. Soc.*, 1995, **78**, 2271–2273.
19. Kim, D. W., Shin, S. I., Lee, J. D. and Oh, S. G., Preparation of chromia nanoparticles by precipitation–gelation reaction. *Mater. Lett.*, 2004, **58**, 1894–1898.
20. Balachandran, U., Siegel, R. W., Liao, Y. X. and Askew, T. R., Synthesis, sintering and magnetic properties of nanophase Cr<sub>2</sub>O<sub>3</sub>. *Nanostruct. Mater.*, 1995, **5**, 505–512.
21. Galeener, F. L., Band limits and the vibrational spectra of tetrahedral glasses. *Phys. Rev. B*, 1979, **19**, 4292–4297.
22. Murakami, Y., Sawata, A. and Tsuru, Y., Crystallisation behaviour of amorphous solid solution and phase separation in the Cr<sub>2</sub>O<sub>3</sub>–Fe<sub>2</sub>O<sub>3</sub> system. *J. Mater. Sci.*, 1999, **34**, 951–955.